Microporous Carbon Membranes from Sulfonated Poly(phthalazinone ether sulfone ketone): Preparation, Characterization, and Gas Permeation

Bing Zhang,[1] Yonghong Wu,[1] Tonghua Wang,[2] Jieshan Qiu,[2] Shouhai Zhang[2]

[1]*School of Petrochemical Engineering, Shenyang University of Technology, 30 Guanghua Street, Liaoyang, Liaoning 111003, China*
[2]*Carbon Research Laboratory, Center for Nano Materials and Science, State Key Lab of Fine Chemicals, School of Chemical Engineering, Dalian University of Technology, Dalian, Liaoning 116012, China*

Received 31 October 2009; accepted 30 January 2011
DOI 10.1002/app.34261
Published online 20 May 2011 in Wiley Online Library (wileyonlinelibrary.com).

ABSTRACT: Microporous carbon membranes (MCM) were prepared from sulfonated poly(phthalazinone ether sulfone ketone) (SPPESK) through stabilization and pyrolysis processes. The effects of sulfonation degree (SD) of SPPESK and the stabilization temperature on the structure and gas permeation of MCM were investigated. The thermal decomposition behavior of SPPESK was studied by thermogravimetric analysis-mass spectrometry. The evolution of functional groups on membrane surface was detected by Fourier transform infrared spectroscopy during heat treatment. The resultant MCM was characterized by X-ray diffraction, Raman spectroscopy, nitrogen adsorption technique and pure gas permeation test (including the gases of H_2, CO_2, O_2, and N_2), respectively. The results have shown that the removal of sulfonic acid groups in SPPESK leads to a weight loss stage in the temperature range of 250–450°C. The surface area, maximum pore volume, and gas permeability of MCM increase with the SD increasing from 59 to 75%, together with the reduction of selectivity. Similarly, the gas permeability of MCM also increases with elevating the stabilization temperature from 350 to 400°C at the loss of selectivity. © 2011 Wiley Periodicals, Inc. J Appl Polym Sci 122: 1190–1197, 2011

Key words: microstructure; pyrolysis; membranes; gas permeation

INTRODUCTION

The increasing demand for "clean," low cost and efficient gas separation technology has resulted in global interest to develop membrane separation technology.[1] Because of the fact that the gas separation performance of membranes is directly connected with the chemical, thermal, and mechanical properties of intrinsic membrane materials, it has become an everlasting hot topic to successively develop new membrane materials with high performance.[1,2] The most promising gas separation membrane materials are capable of operating under harsh conditions while maintaining their efficiency.[3] Microporous carbon membranes (MCM) is one kind of these newly developed membrane materials during the last two decades. They have outstanding gas separation performance, as well as better thermal and chemical stability than traditional polymeric materials.[4] These advantages provide MCM with enormous potential in a wide variety of gas separation applications, such as the recovery or removal of hydrogen, helium, carbon dioxide, air and organic vapors from gas mixtures, as well as catalytic membrane reactors.[5–7] Unfortunately, to date MCM has not yet be widely commercialized due to some unresolved problems, such as the choice of suitable precursors, the complicated mechanism of porous structure formation, low permeability, and high fabrication cost, although great efforts have been taken as reported in literature.[4,5] In the case of precursors, a large number of polymeric materials, including polyimide (PI) and their derivatives,[8] polyfurfuryl alcohol (PFA),[9] cellulose,[10] polyacrylonitrile (PAN),[11] phenol formaldehyde,[12] poly(vinylidene chloride-*co*-vinyl chloride) (PVDC-AC),[13] polyphenylene oxide,[14] etc., have been reported to prepare MCM. However, the gas separation performance of their MCM exhibits big difference due to their various thermal degradation behaviors and porous structure formation mechanisms. In addition, a supported carbon membranes

Correspondence to: B. Zhang (bzhangdut@163.com) and T. Wang (wangth@dlut.edu.cn).

Contract grant sponsor: National Natural Science Foundation of China; contract grant numbers: 20906063, 20276008.
Contract grant sponsor: Liaoning Provincial Natural Science Foundation; contract grant number: 20102170.
Contract grant sponsor: Scientific Research Foundation of Education Department of Liaoning Province; contract grant number: 2008498.

should also consider the effects of support on membrane formation (e.g., micro-crack) and permeation performance.[15]

Generally speaking, the porous structure formation of MCM can be divided into two stages during pyrolysis. At the first stage (usually in the temperature range of 200–500°C), thermal degradation reactions (such as side-group elimination, random scission, and depolymerization, etc.[16]) take place, leading to the formation of amorphous carbon. As the result, the initial porous structure of MCM is generated by the random stacking of amorphous carbons.[17] During this stage, the gas permeability of MCM increases with elevating the pyrolytic temperature. When the pyrolysis progresses to the second stage (during the temperature range of 500–1100°C), with the bourgeoning of graphite-like carbon, the rearrangement and reorganization of graphitic carbon gradually dominate the evolution of porous structure of MCM in stead of the thermal degradation reactions. During this stage, the gas permeability generally slows down with increasing the final pyrolytic temperature. The morphology of resultant porous structure of MCM is constructed by intertwining channels containing relatively wide openings with narrow constrictions. The openings contribute the major part of the pore volume and are responsible for the permeation capacity, while the constrictions hinder the passage of larger molecules in a mixture and are responsible for the selectivity.[5,18] Through the microporous structure, gases can be effectively distinguished from mixtures by their size and shape. Therefore, the gas separation performance of MCM could be modified through the control of the microporous structure by adjusting the chemical structure of precursors and preparation conditions.

Zhou et al. markedly increased the gas permeability of MCM through increasing the content of decomposable sulfonic acid groups in precursor phenolic resin molecular chain.[19,20] Islam et al. significantly improved the gas permeability of MCM by adopting polyimide containing pendent sulfonic acid groups as precursor at lower pyrolytic temperature (from 250 to 450°C).[21] Xiao et al.[22] and Park et al.[23] also increased the gas permeability of MCM by introducing larger groups to molecules and changing the bridging linkage in dianhydride monomer of precursor polyimides, respectively. Yoshimune et al. remarkably enhanced the gas permeability of CO_2 and O_2 without affecting the selectivity by incorporation of transition metal ions such as Ag^+ and Cu^{2+} into poly(phenylene oxide)-based MCM.[24] Park et al. led to a drastic increment in the gas permeability of MCM containing silica from poly(imide siloxane) at a loss of selectivity.[25] Park et al.[26] demonstrated an effective route to obtain dense polymer polyimide film with outstanding molecular and ionic transport and separation performance through rational tailoring of free-volume element architecture (such as pores and channels) by thermally driven segment rearrangement between 350 and 450°C. Kim et al.[27] found that the gas permeability through metal doped carbon membranes increased and the gas selectivity decreased with increasing the diameter or the contents of substituted metal ions in the metal-substituted (including Li^+, Na^+, and K^+) sulfonated polymide precursors.

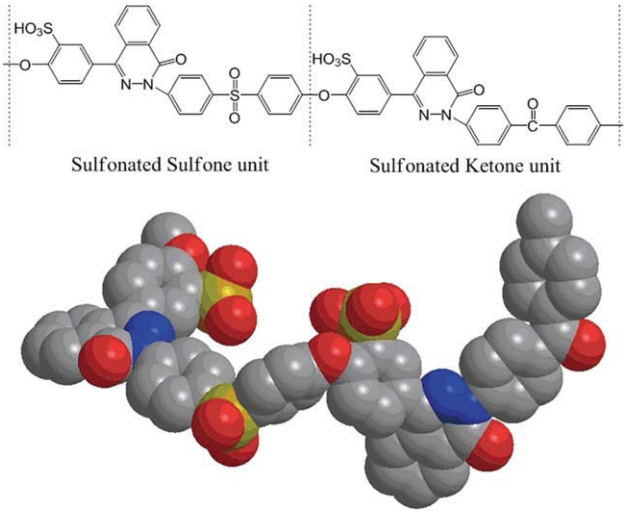

Figure 1 Schematically chemical structure of SPPESK with the sulfonation degree of 200%. [Color figure can be viewed in the online issue, which is available at wileyonlinelibrary.com.]

In our previous work, poly(phthalazinone ether sulfone ketone) (PPESK) has been successfully developed as a kind of promising precursor, from which the best ideal O_2/N_2 separation factor reaches to above 24 for the MCM prepared at the pyrolytic temperature of 800°C.[28] Here, sulfonic acid groups were introduced to PPESK molecular chain to explore their effects on the microstructure and gas permeation property of MCM.

EXPERIMENTAL

Materials synthesis

PPESK, with the molar ratio of sulfone over ketone units of 1 : 1, was kindly supplied by Dalian Polymer New Material Corp. of China. The synthesis of SPPESK was based on the poly(phthalazinone ether sulfone ketone) (PPESK) by the substitution of sulfonic acid groups according to the method reported in pervious article.[29] The sulfonation degree (SD) of SPPESK is determined by acid and base titration. Figure 1 shows the schematically chemical structure of SPPESK created by ChemOffice software. In this work, SPPESK with the SD of 59 and 75% were

synthesized and used as precursors for making MCM. Compared with PPESK, SPPESK possesses better solubility and hydrophilicity due to the strong polarity of -SO_3H and hydrogen bonding.[30] The introduction of bulky sulfonic acid groups will provide more steric hindrance to intersegmental rotation of polymer chain, which is helpful to form MCM with more porous and less compact structure. In addition, the pendent sulfonic acid groups are thermally labile, which would be escaped from the carbonaceous backbone of SPPESK during the early stage of heat treatment. Consequently, the microporous structure and gas separation performance of MCM could be expectantly tuned by the introduction of sulfonic acid groups.

Membrane preparation

First, SPPESK was dissolved in *N*-methyl-2-pyrrolidone (NMP) to make a solution at the concentration of 10 wt %. Then, the solution was poured onto horizontally sanitary glass plates. Yellowish polymeric membranes were formed after the solvent evaporation at 60°C for 2 h and 100°C for 12 h. The obtained polymeric membranes were not further dried to keep a small portion of solvent in the matrix because that a quite dried polymeric membrane is very fragile and difficult to handle at the later steps. To prevent the polymeric membranes from melting during the subsequent pyrolysis, a stabilization process was undertaken at 350 or 400°C for 30 min in the air. Pyrolysis was performed in a tubular furnace that was ramped to 650°C at a rate of 1°C/min in flowing argon, and then was kept at 650°C for 60 min before cooling down to room temperature. The as-prepared homogeneous MCM with the thickness around 20 μm was sealed in a vacuum desiccator to avoid the influence of water vapor and other gases. The MCM was designated as CM(*x*-*y*), where *x* and *y* represent the SD of SPPESK and stabilization temperature, respectively.

Characterization

Thermogravimetric analysis-mass spectrometry (TGA-MS) of SPPESK was undertaken on a NETZSCH STA449C thermogravimetric analyzer connected to a Balzers MID mass spectrometer. The TGA analysis was conducted in flowing nitrogen at a heating rate of 10°C/min from ambient temperature to 800°C. Ion currents at *m/z* equaling to 18, 43, 44, 48, 64, and 78 were detected in on-line measurements to monitor the possible evolved gases during pyrolysis, such as H_2O, C_3H_7-, CO_2, O_3, SO_2, and C_6H_6, etc.

The evolution of functional groups on membrane surface was monitored by a Nexus 470 Attenuated Total Reflection Fourier Transform infrared spectroscopy (ATR-FTIR) (Thermo-Nicolet) in the wavenumber range of 4000–680 cm^{-1}, which was analyzed with OMNIC software.

X-ray diffraction (XRD) patterns were recorded using a D/Max-2400 diffractometer with CuKα radiation in the range of diffraction angle 2θ from 5 to 60° with the scanning step of 0.02°. The indicator of interlayer distance d_{002} of samples was calculated by the well-known Bragg equation.

Raman spectra (500–1800 cm^{-1}) were collected on a Renishaw2000 spectrometer with 514 nm laser excitation and a CCD detector, operating at a power of 100 mW. Spectra were averaged over 5 scans and recorded at a resolution of 1 cm^{-1}. Raman spectrometry is commonly used to characterize the microstructure of carbon materials due to its convenient *La* measurement from the intensity of Raman D-band (disordered or amorphous structures) and G-band (graphitic structures) using an empirical equation, $L_a = 4.35\ (I_G/I_D)$ (nm).[31]

Nitrogen adsorption isotherms of MCM were measured on an ASAP 2020*N* analyzer at −196°C. Prior to the adsorption measurements, all samples were degassed at 200°C for at least 6 h. The pore size distribution and porous parameters (such as BET surface area, maximum pore volume, etc.) were calculated by H-K method based on the adsorption isotherms.[32]

Pure gas permeation of membranes was tested by conventional variable volume-constant pressure method according to the previous reports.[28,33] The permeability *P*, within ± 10% in precision, was obtained from the flux of the tested pure gas on the permeating side, normalized by the partial pressure difference of the gas across the membrane, the effective permeating area and thickness of the membrane. The ideal selectivity α is obtained from the ratio of two pure gas permeabilities,

$$\alpha_{O_2/N_2} = \frac{P_{O_2}}{P_{N_2}} \quad (1)$$

where P_{O_2} and P_{N_2} are the permeabilities for gas O_2 and N_2, respectively. Replicative experiments for each membrane were performed at least three times to ensure good reproducibility. All the gas permeation data present in this paper are referred to the average value.

RESULTS AND DISCUSSION

Thermal degradation behavior

The thermal degradation curve of SPPESK with the SD of 75% and the mass spectra of some evolved gases are shown in Figure 2. For guidance, the

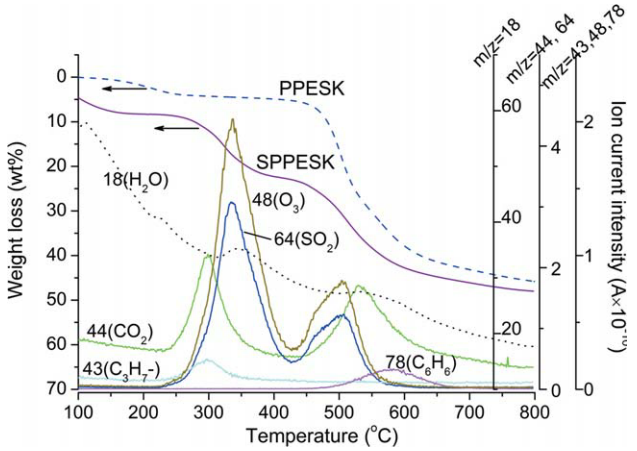

Figure 2 Thermal degradation curve of SPPESK and the mass spectra of evolved gases during pyrolysis. Note: the TGA curve of PPESK was taken from Ref. 28. [Color figure can be viewed in the online issue, which is available at wileyonlinelibrary.com.]

thermal weight loss profile of PPESK is also given on this figure, which is taken from Ref. 28. Their differences in weight loss were not further compared since they were obtained from different drying conditions. Besides the common three weight loss stages for SPPESK and PPESK (~ 250°C, 450–650°C, and 650–800°C), SPPESK has an additional stage during the temperature range of 250–450°C. Prior to the temperature of 250°C, SPPESK successively reduced in weight loss from the onset (beneath 100°C) of thermal degradation measurement due to the release of large amount of absorbed water and residual solvent NMP (bp 202°C) in membrane matrix. At 250°C, the weight loss of SPPESK is 8.8 wt %. When the temperature surpasses 250°C, another significant thermal weight loss occurs for SPPESK, accompanying with the release of large amount of SO_2 and CO_2, as well as small amount of intermediates O_3 and propyl group C_3H_7-. The release amount of CO_2 and C_3H_7- reach their maximum values at the temperature about 300°C, while those of O_3 and SO_2 are around 335°C. It infers that the C—O bonds first rupture between the two adjacent benzene rings in sulfone and ketone units due to its lower bonding energy.[34] The variation trend of H_2O and SO_2 signals detected from mass spectra is very close to the report in literature.[19,21] The evolved gases SO_2 and H_2O above 250°C can be mainly ascribed to the sulfonic acid groups in SPPESK. During the temperature range of 250–450°C, some intermediates are also produced, such as O_3 and C_3H_7- free radical. The presence of O_3 and C_3H_7- free radical maybe promote the scission of C—O and C—S bonds in SPPESK.[18] The successive release of large amount of H_2O can also be partly ascribed to the decomposition of hydrogen bonds that is commonly formed intra- or inter- molecular chains containing sulfonic acid groups.[35] At 335°C, the ion current intensities of H_2O and SO_2 attain their peak values, revealing that intensive decomposition reactions happen to sulfonic acid from molecular chain. When the thermal degradation temperature reaches to 450°C, the weight loss of SPPESK is 24.0%. During the third stage (450-650°C), another remarkable weight loss range takes place. Seen from the MS spectrum, the signals of SO_2, O_3 and CO_2 also reach another peak values about 500-530°C. When the temperature is higher than 500°C, the weight loss of SPPESK is almost in the same trend with that of PPESK. In addition, a signal at *m/z* equaling 78 was observed between 500°C and 650°C, which can be subjected to the isolated benzene rings deduced during the thermal degradation. As the temperature goes up to 650°C, the weight loss of SPPESK has reached about 45.0 wt %. During the fourth stage (650-800°C), the weight loss curve tends to be flat with a little of weight loss contributed by the reorganisation and rearrangement of carbon matrix. At the final temperature of 800°C, the weight loss of SPPESK is about 48.0 wt %. Therefore, the introduction of sulfonic acid groups to PPESK (i.e., SPPESK) has changed the thermal degradation behavior and would undoubtedly modify the microstructure of resultant MCM.

ATR-FTIR spectra

Figure 3 gives the change in functional groups of SPPESK with SD of 75% during the process of carbon membrane formation. In the spectrum of polymeric membrane sample [Fig. 3 (a)], the characteristic reflection appeared clearly, such as the stretching vibrations of C=O (1663 cm^{-1}), the C=N (1589

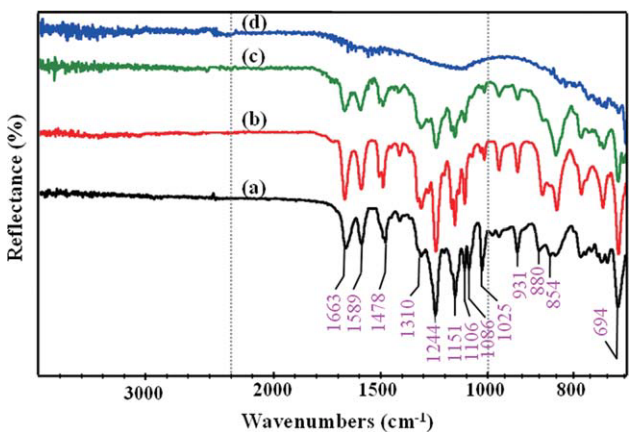

Figure 3 ATR-FTIR spectra of SPPESK with SD of 75% membrane samples through heat treatment: (a) polymeric membranes; (b), (c) stabilized membranes at 350°C and 400°C; and (d) carbon membranes CM(75–350). [Color figure can be viewed in the online issue, which is available at wileyonlinelibrary.com.]

cm^{-1}), the benzene ring (1478 cm^{-1}), the asymmetric and symmetric stretching vibration for sulfone groups (1310 and 1151 cm^{-1}), the ether linkage in C—O—C or=C—O—C groups (1244 and 1106 cm^{-1}), the asymmetrical and symmetrical stretching of O=S=O in -SO_3H groups (1086 and 1025 cm^{-1}), etc. This analysis is well consistent with the typical chemical structure of SPPESK as shown in Figure 1. After stabilization process [Fig. 3(b)], two reflection peaks at 1086 and 1025 cm^{-1} become very weak. It demonstrates that large amount of the -SO_3H groups have been peeled off from the main chain of SPPESK molecules at 350°C. This conclusion is well agreed with the TGA-MS results. In addition, the peak intensities at 974 and 830 cm^{-1} become stronger, which reflect the —C—O—C— asymmetric stretching in four- and three-membered heterocyclic rings, respectively. This indicates that crosslinkings, such as heterocyclic ether-like structure, have been formed intra- or intermolecules after stabilization. When stabilized at 400°C, the spectrum profile of SPPESK is almost intact compared with the sample stabilized at 350°C. Nevertheless, the background of spectrum broadens and all the peak intensity weakens. It can be ascribed to the further decomposition of -SO_3H and C—O groups from molecular at 400°C as illustrated in TG-MS. In the case of carbon membranes [Fig. 3 (d)], all the bands almost disappeared except for aromatic structure. It infers that nonaromatic atoms gradually decompose from the matrix in the form of gases as detected in TGA-MS. The residual structure would be simultaneously combined and reorganized, leading to the formation of more condensed aromatic structure, i.e., graphite-like structure. The disordered stacking of graphite-like structure, such as carbon sheet, amorphous carbon, etc., forms the porous structure (voids and porosity) of carbon membranes for gas permeation.

X-ray diffraction

Figure 4 shows the X-ray diffraction patterns of MCM prepared by different SD in SPPESK and stabilization temperature. There are two diffraction peaks in each pattern of them. The peaks at the 2θ about 21–23° and 43–44° are due to the (002) and (100) planar diffractions, respectively. The present two broad peaks suggest the lower graphitization degree of MCM. In another word, the proportion of amorphous carbon is still at a rather high level. This is similar to the analysis of MCM from other precursors reported in literature, such as Kapton polyimide[36] and poly(phenylene oxide),[37] etc. Although the d_{002} values of carbon materials could not directly yield information that can be interpreted as micropore dimensions, they can serve as the average spacing indicators between the individual layers of the

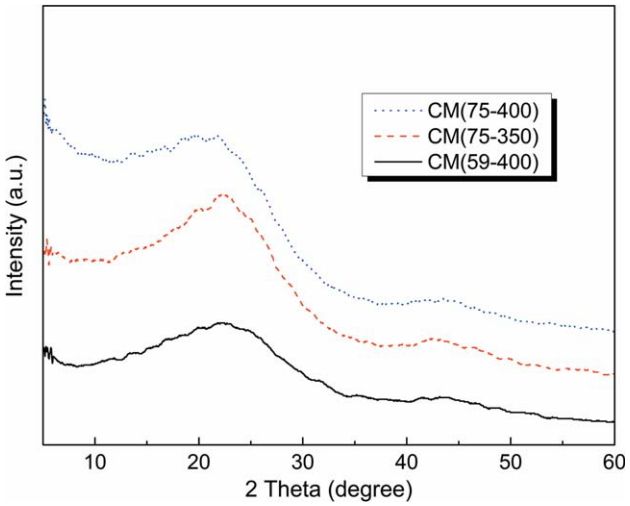

Figure 4 XRD patterns of MCM prepared from SPPESK. [Color figure can be viewed in the online issue, which is available at wileyonlinelibrary.com.]

graphitic carbon. The d_{002} values of carbon materials measured by XRD are commonly used as not only the average interlayer distance of aromatic plane in amorphous carbon but also the indicator of the portion of amorphous carbon in matrix. Because the void volume of MCM is mainly contributed by the amorphous carbon, there will be a quantitative relationship between the d_{002} values and gas permeation properties. However, it needs to be further investigated in detail. The d_{002} values of MCM prepared in the present work is in the range of 4.02–4.07 Å that is slightly higher than that of PPESK-based MCM (4.01 Å) at the same pyrolytic temperature.[38] It implies that the SPPESK-based MCM possesses lower density and less compact structure. However, the structure information obtained from XRD is very limited due to the slight variation of d_{002} values between the samples. Therefore, Raman spectra were also used to further testify the changes in carbon structure of MCM.

Raman spectra

Figure 5 gives the spectra of carbon membrane samples CM(75–400), CM(75–350), and CM(59–400). For all carbon membranes, two peaks can be found centered around the 1350 cm^{-1} and 1580 cm^{-1}, reflecting the D peak (disordered or amorphous structures) and G peak (graphitic structures), respectively. As suggested, the changes in the I_D/I_G ratio could reflect the fraction variation of amorphous carbon and graphitic carbon. The domain size L_a would also be calculated from empirical equation proposed by Tuinstra et al.,[31] as inserted in Figure 5. With increasing the stabilization temperature (i.e., CM(75–350) to CM(75–400)), the L_a value decreases from

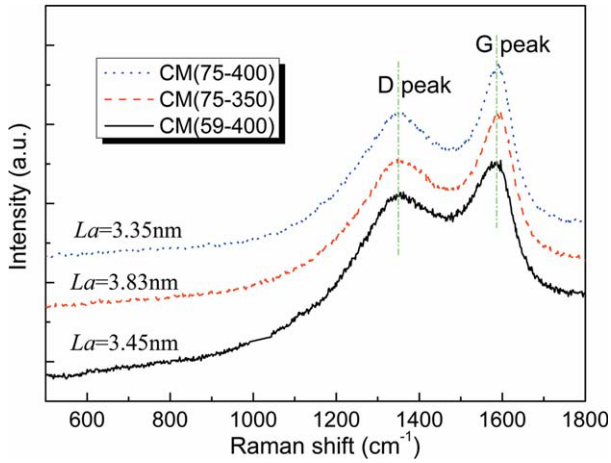

Figure 5 Raman spectra of carbon membranes. [Color figure can be viewed in the online issue, which is available at wileyonlinelibrary.com.]

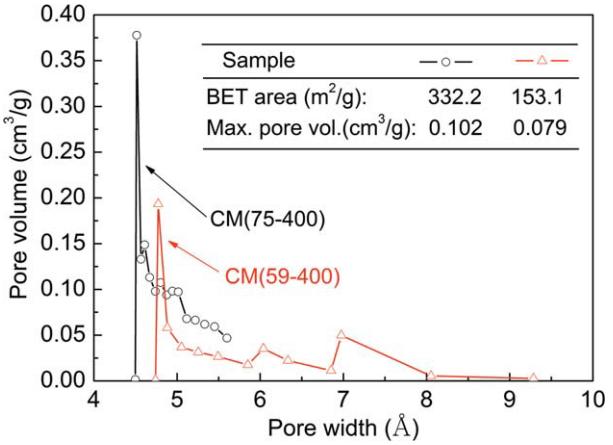

Figure 6 Pore size distributions of MCM by H-K method from nitrogen adsorption technique. [Color figure can be viewed in the online issue, which is available at wileyonlinelibrary.com.]

3.83 nm to 3.35 nm. In addition, with increasing the SD in SPPESK from 59 to 75%, the L_a value decreases form 3.45 nm to 3.35 nm. For carbon materials, their L_a values (or micro-domain size) will become larger and larger as graphitization degree elevated. So it deduces that the graphitization degree of MCM will be improved by increasing stabilization temperature or decreasing SD in SPPESK.

Nitrogen adsorption

To insight into the porous structure of SPPESK-based MCM, nitrogen adsorption technique was applied to characterize the pore size distribution as shown in Figure 6. Although the measurement of nitrogen adsorption is not accurate enough to characterize the complete porous information of microporous carbon membranes because the nitrogen molecules are too large to enter the smaller pores in the membrane structure, it can also give some indicative information on the overall porosity of carbon membranes. The BET surface area and maximum pore volume of samples are also listed in Figure 6. The values are comparable to those of carbon membranes in literature reports.[39–42] Compared CM(75–400) with CM(59–400), higher SD in SPPESK leads MCM to higher BET surface area (i.e., 332.2 m^2/g and 153.1 m^2/g) and larger maximum pore volume (i.e., 0.102 cm^3/g and 0.079 cm^3/g). In another word, the porosity of MCM increases with elevating the SD in SPPESK. Therefore, the gas permeability of MCM could be expectedly enhanced by increasing the SD in SPPESK.

Gas permeation test

Table I lists the gas permeation properties of MCM. With increasing the SD in SPPESK, the gas permeability of the resultant MCM improves, e.g., the O_2 permeability of 30 Barrer for CM(59–400) increasing to 52 Barrer for CM(75–400). However, the selectivity of them simultaneously reduces, e.g., the O_2/N_2 changes from 12 to 8.0. The effect of SD on the gas permeability of MCM is due to the sulfonic acid groups causing additionally more weight loss and loose carbon structure. It indicates that the pendent sulfonic acid groups in SPPESK could take a "template-like" effect on pore-forming in carbon membrane during pyrolysis. This conclusion is also proved by the results and analysis from nitrogen adsorption technique. Higher stabilization temperature is also helpful for improving the gas permeability of MCM, e.g., the O_2 permeability of CM(75–400) being 33.1% higher than that of CM(75–350). The effect of stabilization temperature is probably owing

TABLE I
Gas Permeation of MCM Derived from SPPESK (Measured at 30°C and 0.1 MPa)

	Permeability[a]				Ideal selectivity		
Sample	H_2	CO_2	O_2	N_2	H_2/N_2	CO_2/N_2	O_2/N_2
CM(59-400)	200	120	30	2.5	80	48	12
CM(75-400)	240	160	52	6.4	38	25	8.0
CM(75-350)	150	140	35	3.4	43	41	10

[a] 1 Barrer = 1×10^{-10} cm^3 (STP) cm/cm^2 s cmHg = 3.35×10^{-16} mol m/m^2 s Pa.

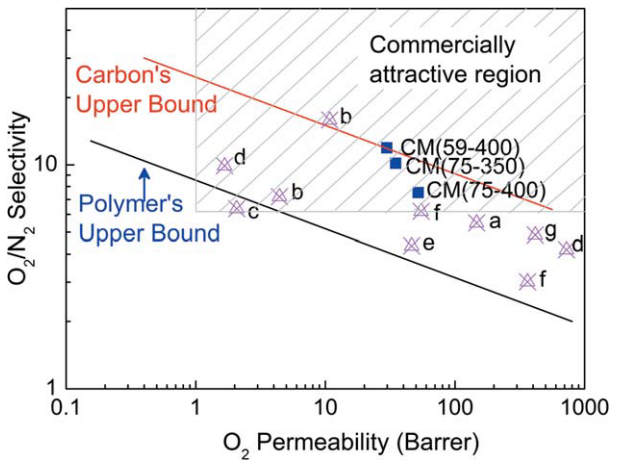

Figure 7 Correlation of permeability with selectivity of MCM for O_2/N_2 system. Notes: a. PPES;[48] b. PPESK;[28] c. phenolic resin;[49] d. poly(furfuryl alcohol);[50] e. polyimide;[51] f. polyimide[52] and g. polyimide.[53][Color figure can be viewed in the online issue, which is available at wileyonlinelibrary.com.]

to the thermal degradation degree because higher stabilization temperature in oxidative atmosphere would cause the matrix of original SPPESK polymeric membranes excessive degradation, which results into more weight loss and less compact structure. This is well in accordance with the results of TGA-MS and Raman. However, the change tendency of selectivity for MCM is opposite to that of permeability. This trade-off relationship between permeability and selectivity is a most common case for all membrane materials.[43]

To evaluate the gas separation performance of MCM from SPPESK, the recommended upper bounds for O_2/N_2 system of polymer and carbon materials are shown in Figure 7.[43,44] As reported, most MCM locate in the region between the two upper bounds and few can surpass the carbon's upper bound getting more commercial competition. From Figure 7, it can be clearly found that all the correlation points of O_2 permeability against O_2/N_2 selectivity of MCM obtained in the present work fall in the hatched region around the carbon's upper bound that is most commercially attractive. It demonstrates that the SPPESK is comparable with other high-performance precursors in literature, such as PPES,[48] PPESK,[28] phenolic resin,[49] poly(furfuryl alcohol)[50] and polyimide.[51–53] It is specially pointed out that the CM(59–400) has lied on the upper bound for MCM that is uncommon. The present work makes us believe that SPPESK is a very promising precursor to prepare MCM with good gas separation performance and the gas permeation of MCM could be well tuned by altering SD in SPPESK or the stabilization temperature.

CONCLUSIONS

MCM was successfully prepared from sulfonated poly(phthalazinone ether sulfone ketone) (SPPESK) through stabilization and pyrolysis. Compared with PPESK, SPPESK has an additional weight loss stage in the temperature range of 250–450°C due to the decomposition of pendent sulfonic acid groups during heat treatment. The microstructure of MCM becomes less compact and higher pore volume with increasing the SD from 59 to 75% or the stabilization temperature from 350 to 400°C. The O_2 permeability of MCM increases from 30 Barrer to 52 Barrer, along with the O_2/N_2 selectivity decreasing from 12 to 8.0, with the SD in SPPSK increasing from 59 to 75%. Similarly, the O_2 permeability of MCM also increases from 35 Barrer to 52 Barrer, along with the O_2/N_2 selectivity decreasing from 10 to 8.0, with the stabilization temperature improving from 350 to 400°C. SPPESK is a competitive precursor in comparison with other precursors (such as PPESK, phenolic resin, poly(furfuryl alcohol) and polyimide) in regard of the gas separation performance of their MCM.

References

1. Freemantle, M. Chem Eng News 2005, 83, 49.
2. Maier, G. Angew Chem Int Ed 1998, 37, 2960.
3. Koros, W. J.; Mahajan, R. J Membr Sci 2000, 175, 181.
4. Saufi, S. M.; Ismail, A. F. Carbon 2004, 42, 241.
5. Ismail, A. F.; David, L. I. B. J Membr Sci 2001, 193, 1.
6. Ockwig, N. W.; Nenoff, T. M. Chem Rev 2007, 107, 4078.
7. Itoh, N.; Haraya, K. Catalysis Today 2000, 56, 103.
8. Jones, C. W.; Koros, W. J. Carbon 1994, 32, 1419.
9. Shiflett, M.; Foley, H. C. Science 1902 1999, 285.
10. Grainger, D.; Hägg, M.–B. J Membr Sci 2007, 306, 307.
11. David, L. I. B.; Ismai, A. F. J Membr Sci 2003, 213, 285.
12. Centeno, T. A.; Vilas, J. L.; Fuertes, A. B. J Membr Sci 2004, 228, 45.
13. Centeno, T. A.; Fuertes, A. B. Carbon 2000, 38, 1067.
14. Lee, H.-J.; Suda, H.; Haraya, K. Sep Purif Technol 2008, 59, 190.
15. Anderson, C. J.; Pas, S. J.; Arora, G.; Kentish, S. E.; Hill, A. J.; Sandler, S. I.; Stevens, G. W. J Membr Sci 2008, 322, 19.
16. Pielichowski, K.; Njuguna, J. Thermal Degradation of Polymeric Materials; Rapra Technology Limited: Shropshire, 2005.
17. Hatori, H.; Yamada, Y.; Shiraishi, M.; Yoshihara, M.; Kimura, T. Carbon 1996, 34, 201.
18. Koresh, J. E.; Soffer, A. Sep Sci Technol 1987, 22, 973.
19. Zhou, W.; Yoshino, M.; Kita, H.; Okamoto, K.–I. Ind Eng Chem Res 2001, 40, 4801.
20. Zhou, W.; Yoshino, M.; Kita, H.; Okamoto, K.–I. J Membr Sci 2003, 217, 55.
21. Islam, M. N.; Zhou, W.; Honda, T.; Tanaka, K.; Kita, H.; Okamoto, K.–I. J Membr Sci 2005, 261, 17.
22. Xiao, Y.; Chung, T.-S.; Chng, M. L.; Tamai, S.; Yamaguchi, A. J Phys Chem B 2005, 109, 18741.
23. Park, H. B.; Kim, Y. K.; Lee, J. M.; Lee, S. Y.; Lee, Y. M. J Membr Sci 2004, 229, 117.
24. Yoshimune, M.; Fujiwara, I.; Suda, H.; Haraya, K. Desalination 2006, 193, 66.
25. Park, H. B.; Jung, C. H.; Kim, Y. K.; Nam, S. Y.; Lee, S. Y.; Lee, Y. M. J Membr Sci 2004, 235, 87.

26. Park, H. B.; Jung, C. H.; Lee, Y. M.; Hill, A. J.; Pas, S. J.; Mudie, S. T.; Wagner, E. V.; Freeman, B. D.; Cookson, D. J. Science 2007, 318, 254.
27. Kim, Y. K.; Park, H. B.; Lee, Y. M. J Membr Sci 2003, 226, 145.
28. Zhang, B.; Wang, T.; Zhang, S.; Qiu, J.; Jian, X. Carbon 2006, 44, 2764.
29. Dai, Y.; Jian, X.; Zhang, S.; Guiver, M. D. J Membr Sci 2002, 207, 189.
30. Dai, Y.; Jian, X.; Liu, X.; Guiver, M. D. J Appl Polym Sci 2001, 79, 1685.
31. Tuinstra, F.; Koenig, J. L. J Chem Phys 1970, 53, 1126.
32. Horvath, G.; Kawazoe, K. J Chem Eng Jpn 1983, 16, 470.
33. Stern, S. A.; Gareis, P. J.; Sinclair, T. F.; Mohr, P. H. J Appl Polym Sci 2035 1963, 7.
34. Nandan, B.; Kandpal, L. D.; Mathur, G. N. Eur Polym Mater 2003, 39, 193.
35. Zhang, S.; Jian, X.; Dai, Y. J Membr Sci 2005, 246, 121.
36. Lua, A. C.; Su, J. Carbon 2006, 44, 2964.
37. Yoshimune, M.; Fujiwara, I.; Haraya, K. Carbon 2007, 45, 553.
38. Wang, T.; Zhang, B.; Qiu, J.; Wu, Y.; Zhang, S.; Cao, Y. J Membr Sci 2009, 330, 319.
39. Lee, H.-J.; Kim, D.-P.; Suda, H.; Haraya, K. J Membr Sci 2006, 282, 82.
40. Lee, L.-L.; Tsai, D.-S. Ind Eng Chem Res 2001, 40, 612.
41. Kim, Y. K.; Park, H. B.; Lee, Y. M. J Membr Sci 2004, 243, 9.
42. Su, J.; Lua, A. C. J Membr Sci 2006, 278, 335.
43. Robeson, L. M. J Membr Sci 1991, 62, 165.
44. Kyotani, T. Carbon 2000, 38, 269.
48. Zhang, B.; Shen, G.; Wu, Y.; Wang, T.; Qiu, J.; Xu, T.; Fu, C. Ind Eng Chem Res 2009, 48, 2886.
49. Kita, H.; Maeda, H.; Tanaka, K.; Okamoto, K.-I. Chem Lett 1997, 179.
50. Shiflett, M. B.; Foley, H. C. J Membr Sci 2000, 179, 275.
51. Fuertes, A. B.; Nevskaia, D. M.; Centeno, T. A. Microporous Mesoporous Mater 1999, 33, 115.
52. Haraya, K.; Suda, H.; Yanagishita, H.; Matsuda, S. Chem Commun 1995, 1781.
53. Okamoto, K.; Kawamura, S.; Yoshino, M.; Kita, H. Ind Eng Chem Res 1999, 38, 4424.